The Astrophysical Journal, 853:92 (8pp), 2018 January 20 https://doi.org/10.3847/1538-4357/aaa1e3

Isotopic and Chemical Evidence for Primitive Aqueous Alteration in the Tagish Lake Meteorite

Keisuke Sakuma[1], Hiroshi Hidaka[1], and Shigekazu Yoneda[2]
[1] Department of Earth and Planetary Sciences, Nagoya University Nagoya 464-8601, Japan
[2] Department of Science and Engineering, National Museum of Nature and Science Tsukuba 305-0005, Japan
Received 2017 April 29; revised 2017 November 28; accepted 2017 November 30; published 2018 January 25

Abstract

Aqueous alteration is one of the primitive activities that occurred on meteorite parent bodies in the early solar system. The Tagish Lake meteorite is known to show an intense parent body aqueous alteration signature. In this study, quantitative analyses of the alkaline elements and isotopic analyses of Sr and Ba from acid leachates of TL (C2-ungrouped) were performed to investigate effects of aqueous alteration. The main purpose of this study is to search for isotopic evidence of extinct ^{135}Cs from the Ba isotopic analyses in the chemical separates from the Tagish Lake meteorite. Barium isotopic data from the leachates show variable ^{135}Ba isotopic anomalies ($\varepsilon = -2.6 \sim +3.6$) which correlatewith ^{137}Ba and ^{138}Ba suggesting a heterogeneous distribution of *s*- and *r*-rich nucleosynthetic components in the early solar system. The ^{87}Rb–^{87}Sr and ^{135}Cs–^{135}Ba decay systems on TL in this study do not provide any chronological information. The disturbance of the TL chronometers is likely a reflection of the selective dissolution of Cs and Rb given the relatively higher mobility of Cs and Rb compared to Ba and Sr, respectively, during fluid mineral interactions.

Key words: meteorites, meteors, meteoroids

1. Introduction

Understanding early alteration processes is important for studying the evolution of the early solar planets. Aqueous alteration is a primitive process that occurred on meteorite parent bodies in the early solar system. In mineralogical studies, the presence of secondary minerals, such as serpentines, oxides, and calcites, in CI and CM chondrites, provides evidence for aqueous activity on parent bodies (Tomeoka & Buseck 1985; Zolensky et al. 1989). Moreover, the chronological and isotopic studies using radioactive decay systems of long- and short-lived nuclides have been widely applied to understand the formation and evolution of solar planetary materials. These techniques were used effectively to put temporal constrains on parent body alteration processes. MacDougall et al. (1984) performed an ^{87}Rb–^{87}Sr chronological study for carbonate formation on the CI chondrite parent body, which identified the timing of precipitation within 100 Ma after the CAI formation. In a chronological study, using ^{53}Mn with a half-life of a 3.7 Ma, the application of a ^{53}Mn–^{53}Cr decay system identified carbonate formation ages in carbonaceous chondrites as 4.3–5.7 Ma after the formation of calcium–aluminum rich inclusions (CAIs), considered to be the earliest condensates in the solar nebula (Fujiya et al. 2012, 2013), which corresponds to the timing of the occurrence of aqueous alteration in primitive solar planets.

In this paper, we focus on the geochemical features of ^{135}Cs, which is extinct nuclide with a half-life of 2.3 Ma (McCulloch & Wasserburg 1978a) estimated from the Ba isotopic analyses of the Tagish Lake (TL) meteorite. The decay system of ^{135}Cs–^{135}Ba is expected to be applicable as a sensitive chronometer for the detection of the aqueous process on the early solar planetary materials because Cs is highly fluid mobile (Hidaka et al. 2001, 2003; Hidaka & Yoneda 2011, 2013; Bermingham et al. 2014, 2016). Previous isotopic studies of Ba in primitive solar materials, however, have not yet been used effectively for chronological applications because of the difficulty detecting radiogenic ^{135}Ba (^{135}Ba*). Considering the large difference in condensation temperature between Cs (799K) and Ba (1455K) (Lodders 2003) and the short half-life of ^{135}Cs, early condensates may provide direct evidence for the decay of ^{135}Cs. Early condensates (e.g., CAIs), however, have low Cs/Ba ratios (CI: 0.0799, Anders & Grevesse 1989 CAIs < 0.00888, Hidaka et al. 2001; Bermingham et al. 2014). Additionally, although high Cs/Ba ratios in materials are essential to find radiogenic ^{135}Ba, it is difficult to find the ideal phases with a high Cs/Ba ratio from early condensates, because of the volatility of Cs. Furthermore, the isotopic compositions of presolar materials have often affected those of primitive materials. In the case of Ba, isotopic excess due to radiogenic ^{135}Ba may be hidden by isotopic anomalies due to *s*-process isotopic enrichments on ^{135}Ba correlated with ^{137}Ba (Hidaka et al. 2001, 2003; Andreasen & Sharma 2007; Carlson et al. 2007; Hidaka & Yoneda 2011, 2013; Bermingham et al. 2014, 2016; Brennecka & Kleine 2017). Previous Ba isotopic studies of sequential leaching experiments of CI and CM chondrites greatly contribute to our understanding of isotopic anomalies in the early solar system. These data suggest the presences of several additional nucleosynthetic components (Hidaka et al. 2001, 2003; Carlson et al. 2010; Hidaka & Yoneda 2011, 2013). In particular, large isotopic deficits of ^{135}Ba and ^{137}Ba showing enrichment of *s*-process components are obtained from the acid residues in CI and CM chondrites. This result is consistent with the Ba isotopic data directly from presolar SiC in the acid residue of the Murchison meteorite, which showed enrichment of *s*-process isotopes (Ott & Begemann 1990; Prombo et al. 1993).

From a chemical and isotopic standpoint, the TL meteorite is similar to CI and CM chondrites (Brown et al. 2000; Clayton & Mayeda 2001; Friedrich et al. 2002). The mineralogical studies of TL show the presence of secondary minerals, such as serpentine and calcite, which is suggestive of intensive aqueous alteration on the TL parent body in the early solar system (Zolensky et al. 2002; Nakamura et al. 2003). The TL meteorite

has lower density and higher porosity than CI and CM chondrite, and is identified as a C2-ungrouped chondrite (Zolensky et al. 2002). The Re-Os systematics and platinum group element measurements provide a model that links TL with CI and CM chondrites to the same parent body (Brandon et al. 2005), but the relationship between three chondrites is still unclear (Hiroi et al. 2001; Vernazza et al. 2013). From spectroscopic studies, it is pointed out that TL originates in D-type asteroids (Hiroi et al. 2001), and there are reports that it is a different origin from CM (Vernazza et al. 2013).

The main purpose of this study is to find isotopic evidence for extinct ^{135}Cs from the Ba isotopic analyses in the chemical separates from the TL meteorite. In the previous study, one of the CM meteorites, the Sayama meteorite is known to contain serpentinized phases in chondrules, which suggests the replacement from olivine by aqueous alteration (Yoneda et al. 2001). Microregion analyses using an ion microprobe revealed the chemical and isotopic heterogeneity of Rb, Sr, Cs, and Ba in the serpentinized parts of a chondrule (Hidaka et al. 2015). The serpentinized phases have higher abundances of Rb and Cs than the other chondrule parts, which suggests that serpentine is one of the specific minerals that selectively adsorbs alkaline elements. Secondary minerals with high abundance of alkaline elements are present in meteorites (Zolensky et al. 1999). The redistribution and selective adsorption of alkaline elements into specific phases possibly occurred in association with aqueous activity. In addition, alkaline elements include several radiogenic nuclides, such as ^{40}K, ^{87}Rb, and ^{135}Cs, which are expected to be used for their decay systems in chronometers. In this paper, we report the chemical and isotopic signatures of the TL meteorite to identify the primitive evolution of the parent body. We are primarily assessing if the results from the redistribution behavior between alkaline and alkaline Earth elements provide any chronological information associated with aqueous alteration in the early solar planetary system.

2. Experimental Methods

2.1. Chemical Treatment

Finding high Cs/Ba phases in a sample is required to establish ^{135}Cs–^{135}Ba chronometry. In this study, a sequential acid-leaching experiment was performed as described previously (Hidaka et al. 2001). About 400 mg of powdered sample was leached using 5 mL of 0.1 M CH_3COOH-CH_3COONH_4, 0.1 M HCl, 2 M HCl, and aqua regia, successively. In each leaching step, the sample was ultrasonicated for 1 hr and kept at room temperature for 23 hr after adding each reagent. The acid residue was finally decomposed by HF–$HClO_4$ for 5 days at 130–150 °C. The complete dissolution was confirmed visually. Separately from the above leaching treatment, about 40 mg of the powdered sample was decomposed by HF–$HClO_4$, and treated as a whole rock for analysis. Each fraction was evaporated to dryness, and redissolved in 2 M HCl of 1 mL. These samples of five leaching fractions and whole rock were designated as L1, L2, L3, L4, L5, and WR, respectively. Each fraction recovered from individual leaching steps was divided into two portions for Sr and Ba isotopic analyses and for the determination of Rb, Sr, Cs, and Ba elemental abundance.

Minor portions (~10% of the total amount) of L1–5 and WR fractions were evaporated to dryness once and redissolved into 5 ml of 2% HNO_3. An Agilent 7700× inductively coupled plasma mass spectrometry was used for the determination of elemental abundances of Rb, Sr, Cs, and Ba.

Major portions (~90%) of L1–5 and WR fractions were used for the isotopic studies after chemical separation with conventional resin chemistry (Hidaka & Yoneda 2014). The method for Sr and Ba chemical separation was carried out as follows: Each sample solution was loaded onto cation-exchange resin packed column (AG50WX8, 200–400 mesh, H^+ form, 50 mm length ×4.0 mm diameter). The column was washed with 3.5 mL of 2 M HCl for the elution of major elements, and then it was washed with 3.5 mL of 2 M HCl for the elution of the Sr fraction. Finally, the column was washed with 2 mL of 3 M HNO_3 for the elution of the Ba fraction. The recover yields of Sr and Ba were more than 90%. The Sr and Ba fractions were evaporated. Sr fractions recovered by the cation-exchange resin method often include Rb, which produces isobaric interference in the Sr isotopic measurement. For further purification, the Sr fraction was loaded onto a Sr-resin packed column (Eichrom, Sr resin, particle size of 100–150 μm, 100 mm length × 2.5 mm diameter). The column was washed with 2.5 mL of 3 M HNO_3 for the elution of Rb, and was washed with 3 mL of ultrapure water for the elution of Sr.

2.2. Sr and Ba Isotopic Analyses

A TRITON-Plus thermal ionization mass spectrometer equipped with nine Faraday cups linked to 10^{11} Ω resistors was used for Sr and Ba isotopic analyses. All analyses were performed in static mode with the amplifier rotation system in use (Hidaka & Yoneda 2013).

The Sr fraction was loaded on a single Re filament with a Ta_2O_5 activator. Strontium has four isotopes: ^{84}Sr is the *p*-process isotope, ^{86}Sr is the *s*-process isotope, and ^{87}Sr and ^{88}Sr are the *s*-process and *r*-process isotopes, respectively. In addition, ^{87}Sr includes radiogenic ^{87}Sr produced from the decay of ^{87}Rb ($t_{1/2} = 4.88$ Ga). Strontium isotopic analyses were performed to monitor the mass not only at ^{84}Sr, ^{86}Sr, ^{87}Sr, and ^{88}Sr, but also at ^{85}Rb to evaluate the isobaric interference of ^{87}Rb for ^{87}Sr. All Sr isotopic data were referenced to ^{86}Sr. For the correction of instrumental mass fractionation, Sr isotopic data were normalized by $^{88}Sr/^{86}Sr = 8.375209$ using the exponential law (Nier 1938). An $^{88}Sr^+$ ion beam of (0.16–16) × 10^{-11} A from 30–2000 ng of Sr loaded on a filament was obtained for more than 5 hr from individual fractions.

The Ba fraction was loaded on the outer filament of a double Re filament assembly, without any activators. Barium isotopic analyses were performed to monitor the mass at ^{130}Ba, ^{132}Ba, ^{134}Ba, ^{135}Ba, ^{136}Ba, ^{137}Ba, and ^{138}Ba in addition to monitor ^{139}La and ^{140}Ce for evaluation of isobaric interferences of ^{138}La, ^{136}Ce, and ^{138}Ce in the Ba mass spectra. During any analyses in this study, detectable interferences from La and Ce were not found. All Ba isotopic data were referenced to ^{136}Ba. For the correction of instrumental mass fractionation, Ba isotopic data was normalized by $^{134}Ba/^{136}Ba = 0.307776$ (Hidaka et al. 2003) using the exponential law. ^{134}Ba and ^{136}Ba are *s*-only process isotopes because *r*-process isotopes of ^{134}Xe and ^{136}Xe are shielded (Hidaka et al. 2003). The normalizing factor of $^{134}Ba/^{136}Ba = 0.307776$ is useful to discuss additional nucleosynthetic components (Hidaka et al. 2003; Hidaka & Yoneda 2011, 2013). A $^{138}Ba^+$ ion beam of (1.0–14) × 10^{-11} A from 60–3000 ng of Ba loaded on a filament was obtained for more than 5 hr from individual

Table 1
Elemental Abundances (ppb) of Rb, Sr, Cs, and Ba, and Rb/Sr and Cs/Ba Ratios in the Leachates (L1-5) and the Whole Rock (WR) of the TL Meteorite

	Rb	Sr	Cs	Ba	Rb/Sr	Cs/Ba
L1	1440 ± 30	5970 ± 40	56.8 ± 0.7	1430 ± 10	0.241 ± 0.005	0.0398 ± 0.0006
L2	319 ± 5	2270 ± 10	23.4 ± 0.4	1280 ± 20	0.141 ± 0.003	0.0183 ± 0.0004
L3	329 ± 2	1089 ± 5	49.0 ± 0.4	1670 ± 20	0.302 ± 0.002	0.0293 ± 0.0003
L4	141 ± 1	112 ± 2	15.0 ± 0.5	250 ± 7	1.26 ± 0.03	0.060 ± 0.003
L5	640 ± 3	2048 ± 6	15.1 ± 0.2	13590 ± 20	0.312 ± 0.002	0.0011 ± 0.00002
WR	3016 ± 2	11730 ± 10	161.3 ± 0.3	10670 ± 10	0.2570 ± 0.0004	0.01512 ± 0.00003

Note. Analytical errors are shown in 1 S.D. (standard deviations) of runs.

fractions. There are no shifts in isotopic compositions observed when different amounts of Sr and Ba materials were measured.

In this study, chemical reagents (Sr standard solution produced by NIST SRM-987; Ba standard solution produced by SPEX CertiPrep) were used as standard materials for Sr and Ba.

3. Results and Discussion

3.1. Rb/Sr and Cs/Ba Ratios of Leachates, Acid Residue, and Whole Rock

Rubidium, Sr, Cs, and Ba elemental abundances and Rb/Sr and Cs/Ba elemental ratios of L1–5 and WR fractions are listed in Table 1. The correlation diagram between Rb/Sr and Cs/Ba elemental ratios of L1–5 and WR of the TL sample based on the chemical data given in Table 1 is shown in Figure 1. In this figure, the reference data of the whole rocks of CI and CM chondrites and the TL meteorite are also plotted for comparison (CI from Anders & Grevesse 1989; Friedrich et al. 2002 CM from Friedrich et al. 2002; Yokoyama et al. 2015 TL from Brown et al. 2000; Friedrich et al. 2002; Yokoyama et al. 2015). The CI and CM chondrites and the TL meteorite are known to show evidence for aqueous alteration on their parent bodies in the early solar system. The Cs/Ba ratios of whole rock samples for the TL meteorite and the CI and CM chondrites are more variable than their Rb/Sr ratios (Cs/Ba, 0.011 ∼ 0.085; Rb/Sr, 0.14 ∼ 0.35), which suggests that the Cs/Ba ratio is more sensitive to aqueous activity on a meteorite parent body than the Rb/Sr ratio. This is likely due to the difference in mobility between Cs and Rb in solid and liquid phases. The mobility of the element in solid and liquid phases can be experimentally defined as partition coefficients (K_D). It is reported that the K_D value of Cs in solid and liquid phases shows a larger variation than that of Rb, and that it greatly depends on the type of solids (Sanchez et al. 2002; Sheppard et al. 2009). These data are often used to discuss the long-termed geochemical behaviors of radionuclides in geological media from the view point of radioactive waste disposal, and may also provide a hint to consider the redistribution behaviors of alkaline elements under aqueous activity in this study. Considering the large variations of Rb/Sr and Cs/Ba ratios in the L1–5 fractions collected from TL (Rb/Sr, 0.14 ∼ 1.3; Cs/Ba, 0.0011 ∼ 0.060), the sequential acid-leaching technique used in this study is useful for chronological purposes to collect several phases with the variable Cs/Ba elemental ratio from the whole rock. Our data are consistent with previous studies using the same leaching-procedures to collect a wide range of Cs/Ba fractions in samples (Hidaka et al. 2001, 2003; Hidaka & Yoneda 2011, 2013). The sequential acid-leaching procedure used in this study was partly modified from the previous method (Shima & Honda 1967). The specific phases dissolved in each leachate are speculated to be water-soluble minerals (L1 and L2), olivine (L3), phosphides (L4), and acid-resistant materials (L5) (Shima & Honda 1967; Hidaka et al. 2001). In particular, Cs/Ba ratios of L1, 2, 3, and 4 fractions are higher than that of WR. The results from the whole rock analyses show that the Cs/Ba ratio of whole rock of the TL meteorite (0.011–0.049) is the lowest among other CI (0.080–0.085) and CM (0.031–0.055) chondrites (Figure 1). In previous studies, 0.1 M CH_3COOH-CH_3COONH_4 leachate (L1) show high Cs abundance (Hidaka et al. 2001) and 2M HCl leachates (L3) also show high Cs abundance (Hidaka & Yoneda 2013). It would be reasonable to consider that the Cs/Ba ratios in TL, CI, and CM reflect the magnitude of aqueous alteration on the meteorite parent bodies. The Cs/Ba ratios from the TL leachates are further evidence for intensive aqueous alteration on the TL parent body.

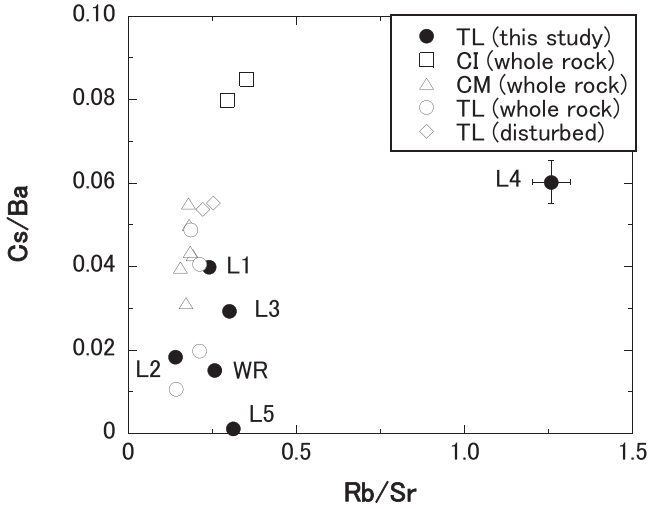

Figure 1. Correlation diagram of the elemental ratios between Rb/Sr and Cs/Ba of L1-5 and WR fractions collected from TL. For the comparison of the data in other primitive meteorites experienced aqueous alteration, the data of whole rocks of CI, CM, and previously studied TL are also shown in the figure (CI, Anders & Grevesse 1989; Friedrich et al. 2002 CM, Friedrich et al. 2002; Yokoyama et al. 2015 TL, Brown et al. 2000; Friedrich et al. 2002; Yokoyama et al. 2015). The data of TL (disturbed) are shown altered parts in TL (Friedrich et al. 2002).

3.2. Sr and Ba Isotopic Data

All of the Sr and Ba isotopic data for the leaching fraction (L1–5) and whole rock (WR) are listed in Tables 2 and 3, respectively. The results of repeated analyses of standard materials for Sr and Ba are also listed in the same tables. The

Table 2
Isotopic Data of Sr in the Standard, L1-5 and WR Fraction of TL

(a)Repeated Analyses of the Standard Material for Sr		
	$^{84}Sr/^{86}Sr$	$^{87}Sr/^{86}Sr$
Sr standard solution		
1	0.0564865 ± 0.0000011	0.710255 ± 0.000002
2	0.0564861 ± 0.0000010	0.710258 ± 0.000002
3	0.0564845 ± 0.0000008	0.710254 ± 0.000002
4	0.0564883 ± 0.0000017	0.710265 ± 0.000003
5	0.0564863 ± 0.0000015	0.710262 ± 0.000003
average	0.0564863	0.710259
External precision (2σ, ppm)	48	13
(b)Samples		
	$\varepsilon^{84}Sr$	$^{87}Sr/^{86}Sr$
L1	0.35 ± 0.23	0.737210 ± 0.000002
L2	0.40 ± 0.24	0.725342 ± 0.000002
L3	1.75 ± 0.38	0.729698 ± 0.000003
L4	0.04 ± 1.52	0.782063 ± 0.000012
L5	−0.97 ± 2.22	0.715547 ± 0.000017
WR	6.04 ± 8.01	0.730789 ± 0.000052
standard		0.710255 ± 0.000002

Note. Sr data are normalized to ^{86}Sr and fractionation corrected to $^{88}Sr/^{86}Sr = 8.375209$ using the exponential law (Nier 1938). The uncertainty of each individual measurement is the internal 2 s.e. of the run. The precision of average value is the 2 s.d. of the average.

data are expressed as relative deviations of the isotopic ratios between samples and individual standard materials in ϵ units defined as follows:

$$\varepsilon\ ^{i}\mathrm{Sr} = \left\{ \frac{(^{i}\mathrm{Sr}/^{86}\mathrm{Sr})\mathrm{sample}}{(^{i}\mathrm{Sr}/^{86}\mathrm{Sr})\mathrm{standard}} - 1 \right\} \times 10^{4}$$

$$\varepsilon\ ^{i}\mathrm{Ba} = \left\{ \frac{(^{i}\mathrm{Ba}/^{136}\mathrm{Ba})\mathrm{sample}}{(^{i}\mathrm{Ba}/^{136}\mathrm{Ba})\mathrm{standard}} - 1 \right\} \times 10^{4}.$$

The Ba isotopic deviation patterns of L1–5 and WR fractions are shown in Figure 2. The WR pattern shows isotopic excess of ^{135}Ba and ^{137}Ba ($\varepsilon^{135}Ba = 0.45 \pm 0.06$ and $\varepsilon^{137}Ba = 0.19 \pm 0.09$). The Ba isotopic data for the CI and CM chondrites also showed isotopic excess of coupled ^{135}Ba and ^{137}Ba ($0 < \varepsilon^{135,137}Ba < 1$), caused by additional nucleosynthetic components of the *r*-process isotopes (Andreasen & Sharma 2007; Carlson et al. 2007) or deficit of nucleosynthetic components of the *s*-process isotope (Bermingham et al. 2016). The Ba isotopic pattern for the whole rock of the TL meteorite was similar to those of the CI and CM chondrites (Andreasen & Sharma 2007; Carlson et al. 2007; Bermingham et al. 2016), which were interpreted to reflect nucleosynthetic components of the *s*- or *r*-process.

On the other hand, the Ba isotopic deviation patterns of L1–5 show variable and large deviations compared with that of WR. The patterns of L1–4 show a variable isotopic excesses of ^{130}Ba, ^{132}Ba, ^{135}Ba, ^{137}Ba, and ^{138}Ba, while that of L5 shows isotopic deficits of ^{130}Ba, ^{132}Ba, ^{135}Ba, ^{137}Ba, and ^{138}Ba.

Isotopic data for several phases collected from leaching experiments in primitive meteorites provide information about isotopic heterogeneity in the early solar systems that cannot be deduced from isotopic data of WR. In previous Ba isotopic studies using leaching experiments in CI and CM chondrites (Hidaka et al. 2001, 2003; Hidaka & Yoneda 2011, 2013), the Ba isotopic data of the acid residues showed large isotopic anomalies because of the enrichment of presolar SiC grains, which is a representative carrier of *s*-process isotopes (Ott & Begemann 1990; Prombo et al. 1993).

To evaluate the additional *s*- and *r*-process nucleosynthetic components from the isotopic anomalies of ^{135}Ba, ^{137}Ba, and ^{138}Ba, the Ba isotopic data in this study were the two-component mixing model between average of solar component and the *s*-process component given by Hidaka et al. (2003). Figures 3(a) and (b) show the correlation diagrams of $\varepsilon^{135}Ba$ versus $\varepsilon^{137}Ba$, and $\varepsilon^{138}Ba$ versus $\varepsilon^{137}Ba$ for measured Ba isotopic data from the chemical separates of TL in this study and theoretical data calculated from the Ba isotopic data of *s*-process components. The Ba isotopic data of *s*-process components are used in the isotopic data of presolar SiC grains (Ott & Begemann 1990; Zinner et al. 1991; Prombo et al. 1993). The shaded zones in the figures indicate the theoretical Ba isotopic data using *s*-process components (Ott & Begemann 1990; Zinner et al. 1991; Prombo et al. 1993). For comparison, the line in Figure 3 indicates mixing the Ba isotopic data between the solar value and additional nucleosynthetic components based on the stellar model (^{135}Ba:^{137}Ba:$^{138}Ba = 34.8$:31.9:33.4; Bisterzo et al. 2015).

The Ba isotopic deviation pattern of acid residue (L5) in the TL meteorite can be explained by a two-component mixing model between the average of the solar and additional nucleosynthetic *s*-process components derived from presolar SiC grains (Ott & Begemann 1990; Zinner et al. 1991; Prombo et al. 1993; Savina et al. 2003; A'vila et al. 2013). It is reasonable that the L5 data point is plotted on the shaded zones in Figures 3(a) and (b), considering that acid-resistant presolar SiC components have survived through the sequential leaching processes, and are enriched in the acid-residual fraction L5.

The Ba isotopic patterns of the L1–4 fractions show variable isotopic excesses (Figure 2). In our previous studies, Ba isotopic data except for ^{130}Ba and ^{132}Ba of leachates in carbonaceous

Table 3
Isotopic Data of Ba in the Standard, L1-5 and WR Fraction of TL

(a)Repeated Analyses of the Standard Material for Ba

	$^{130}Ba/^{136}Ba$	$^{132}Ba/^{136}Ba$	$^{135}Ba/^{136}Ba$	$^{137}Ba/^{136}Ba$	$^{138}Ba/^{136}Ba$
Ba standard solution					
1	0.0134825 ± 0.0000006	0.0129001 ± 0.0000006	0.839309 ± 0.000002	1.429097 ± 0.000005	9.129629 ± 0.00005
2	0.0134816 ± 0.0000004	0.0128983 ± 0.0000004	0.839294 ± 0.000002	1.429100 ± 0.000005	9.129570 ± 0.00004
3	0.0134824 ± 0.0000009	0.0128997 ± 0.0000010	0.839315 ± 0.000003	1.429092 ± 0.000008	9.129456 ± 0.00007
4	0.0134816 ± 0.0000009	0.0128978 ± 0.0000009	0.839299 ± 0.000003	1.429085 ± 0.000007	9.129412 ± 0.00007
5	0.0134812 ± 0.0000008	0.0128992 ± 0.0000009	0.839303 ± 0.000004	1.429094 ± 0.000008	9.129655 ± 0.00007
Average	0.0134819	0.0128990	0.839304	1.429093	9.129545
External precision (2σ, ppm)	85	147	20	8	23

(b)Samples

	$\varepsilon^{130}Ba$	$\varepsilon^{132}Ba$	$\varepsilon^{135}Ba$	$\varepsilon^{137}Ba$	$\varepsilon^{138}Ba$
L1	6.52 ± 1.19	6.24 ± 1.18	3.15 ± 0.07	1.67 ± 0.08	0.58 ± 0.10
L2	3.26 ± 0.79	2.80 ± 0.83	2.96 ± 0.05	1.47 ± 0.07	0.49 ± 0.06
L3	6.59 ± 1.15	5.07 ± 1.21	3.56 ± 0.06	2.02 ± 0.09	0.84 ± 0.12
L4	7.81 ± 7.26	12.25 ± 7.52	2.62 ± 0.26	1.70 ± 0.30	1.21 ± 0.46
L5	−3.81 ± 1.24	−3.12 ± 1.24	−2.64 ± 0.09	−1.37 ± 0.10	−0.67 ± 0.15
WR	1.09 ± 1.17	1.27 ± 1.23	0.45 ± 0.06	0.19 ± 0.09	0.09 ± 0.12

Note. Ba data are normalized ^{136}Ba and fractionation corrected to $^{134}Ba/^{136}Ba = 0.307776$ (Hidaka et al. 2003) using the exponential law. The uncertainty of each individual measurement is the internal 2 s.e. of the run. The precision of average value is the 2 s.d. of the average.

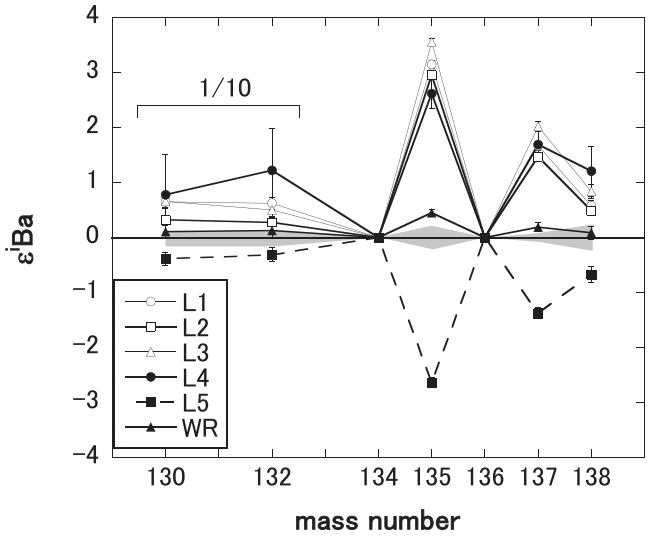

Figure 2. Ba isotopic deviation patterns of L1-5 and WR fractions of TL. The data of ^{130}Ba and ^{132}Ba are plotted in one-tenth of the measured values. Analytical errors are shown in 2σ of the means. The shaded zone in the figure shows external precision as determined from the 2σ of the population of replicate standard measurements.

chondrites could not be explained only from the addition of *s*- and *r*-process nucleosynthetic components (Hidaka et al. 2003; Hidaka & Yoneda 2011, 2013). All six data points in the $\varepsilon^{135}Ba$ versus $\varepsilon^{137}Ba$ diagram (Figure 3(a)) fall in the mixing zone, while three of the six data points from the L1-3 in $\varepsilon^{137}Ba$ versus $\varepsilon^{138}Ba$ diagram (Figure 3(b)) are plotted off the zone. Considering that the ^{138}Ba isotope has the least *r*-process component comprising it, it is unlikely to interpret that the addition of an *r*-process component caused the offset shown in Figure 3(b). As one of the possibilities, there is an addition of radiogenic ^{138}Ba decayed from ^{138}La ($t_{1/2} = 105$ Ga) (Brennecka et al. 2013). Our estimates from the chemical data of La/Ba elemental ratios in the leachates provide the $(^{138}Ba^{*}/^{138}Ba) = 0.4$ to 4.5 ppm, which concludes that the production of $^{138}Ba^{*}$ is not resolvable by the Ba isotopic measurements in the current TIMS techniques. The Ba isotopic data of leachates reveal the existence of several additional nucleosynthetic components that originated not only from acid-resistant SiC but also from acid-soluble materials in the TL meteorite.

3.3. Chronological Application from ^{87}Rb–^{87}Sr and ^{135}Cs–^{135}Ba Decay Systems

The ^{87}Rb–^{87}Sr evolution diagram for the TL meteorite is shown in Figure 4(a). The line in Figure 4(a) is a 4.568 Ga-old reference line corresponding to the formation age of CAIs from the CV3 meteorite (Bouvier & Wadhwa 2010). In the figure, the L2 data point is consistent with the reference line, while the other four data points of L1, L3, L4, L5, and WR fall off the line. The ^{87}Rb–^{87}Sr chronometer of TL might have been disturbed by late activities on the parent body, such as igneous, aqueous, metamorphic, or impact events. It is plausible that the ^{87}Rb–^{87}Sr chronometer had been disturbed by aqueous activity on the TL meteorite parent body, considering the Rb/Sr ratios of the TL L1–5 fractions shown in Figure 1. Less correlation between Rb/Sr and $^{87}Sr/^{86}Sr$ from the sequential leachates as shown in Figure 4(a) is also reported in other primitive chondrites (Qin et al. 2011; Yokoyama et al. 2015). It is reasonable to interpret that Rb and Sr are contained in different phases as the result of chemical redistribution by primitive aqueous alteration, and that they are differentially leached from these phases by the different acids.

The ^{135}Cs–^{135}Ba isochron diagram for the TL meteorite is shown in Figure 4(b). Because all of the Ba isotopic compositions from the TL meteorite suffered from the addition or depletion of nucleosynthetic *s*-process components, it is impossible to detect the presence of radiogenic ^{135}Ba directly from the isotopic compositions. Assuming that the ^{135}Ba isotopic excesses of TL were derived from two origins, the nucleosynthetic *s*-process component and the radiogenic

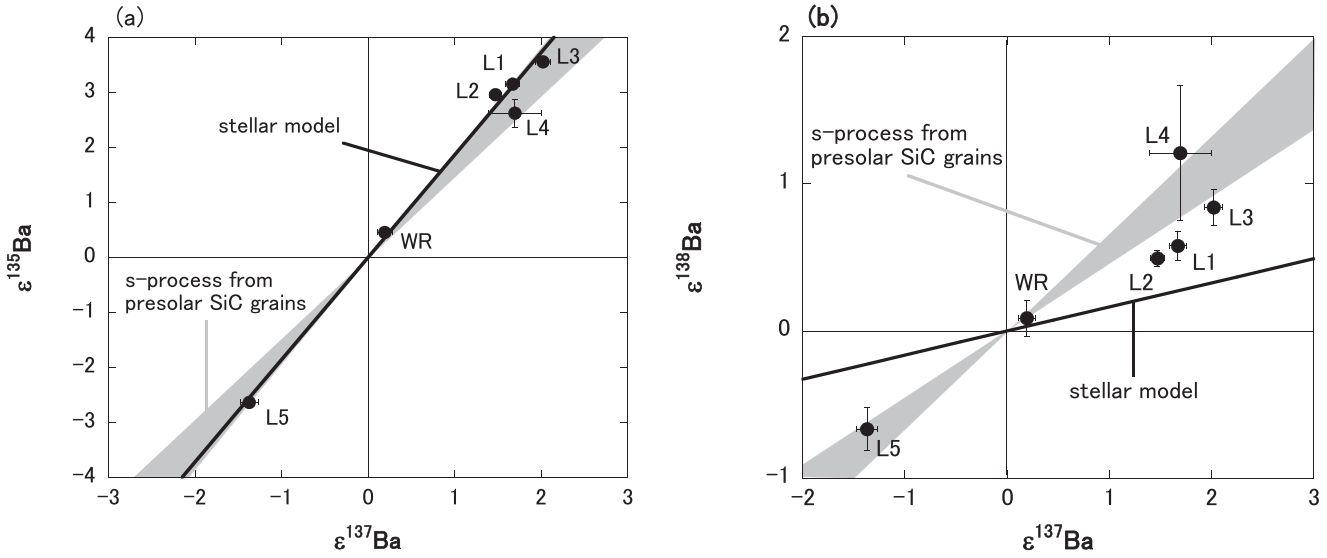

Figure 3. Correlation diagrams of (a) ε^{135}Ba vs. ε^{137}Ba and (b) ε^{138}Ba vs. ε^{137}Ba. For Ba isotopic data in this study and Ba isotopic data calculated two-component mixing between average solar value component and *s*-process component. The gray zones in the figures show mixing zones between the average solar system component and *s*-process component given by isotopic study of presolar SiC grains (Ott & Begemann 1990; Zinner et al. 1991; Prombo et al. 1993). The lines in the figures show the isotopic ratio of the additional nucleosynthetic component calculated by the stellar model (Bisterzo et al. 2015).

component, the amount of radiogenic ^{135}Ba, (ε^{135}Ba*), can be calculated from the subtraction of the additional nucleosynthetic components using the following equation:

$$(\varepsilon^{135}\mathrm{Ba}^*) = (\varepsilon^{135}\mathrm{Ba}) - (\varepsilon^{137}\mathrm{Ba}) \times f,$$

where f is a factor showing the ^{135}Ba/^{137}Ba isotopic ratio of the additional nucleosynthetic *s*-process component (Ott & Begemann 1990; Zinner et al. 1991; Prombo et al. 1993; Savina et al. 2003; Bisterzo et al. 2015). As shown in Figure 3(a), the ^{135}Ba/^{137}Ba isotopic ratio of additional nucleosynthetic components is from 1.517 (f_{min}) to 1.908 (f_{max}), as estimated from the isotopic data from presolar SiC grains (f_{min}: Zinner et al. 1991 f_{max}: Prombo et al. 1993). The ^{135}Cs–^{135}Ba isochron diagram consisting of the Cs/Ba elemental ratios and calculated ε^{135}Ba, (ε^{135}Ba*), of the TL leachates is shown in Figure 4(b). Since there is no positive correlation in the figure, chronological information cannot be provided from the Cs–Ba data set in this study. Although the data set collected in this study is limited, more data collection in the future may refine this approach.

Although there are several studies on ^{135}Cs in the early solar system (McCulloch & Wasserburg 1978a; Hidaka et al. 2001; Hidaka & Yoneda 2011, 2013; Bermingham et al. 2014, 2016; Brennecka & Kleine 2017), the estimated initial ^{135}Cs abundance ranges from 2.8×10^{-6} to 6.8×10^{-4} but is still disputed. The time interval between the formation of CAIs and the occurrence of primitive aqueous alteration was estimated to be 4.3–5.7 Ma from the Mn–Cr dating of carbonates in chondrites (Fujiya et al. 2012). Assuming the initial ^{135}Cs/^{133}Cs ratio ((Brennecka & Kleine 2017) for minimum value $= 2.8 \times 10^{-6}$ and (Hidaka & Yoneda 2013) for maximum $= 6.8 \times 10^{-4}$) and the formation interval of the carbonates, the ^{135}Ba isotopic excesses produced by radiogenic ^{135}Ba of individual TL leaching fractions are estimated as ε^{135}Ba = 0.000073–1.5. Considering the analytical precision for Ba isotopic measurements in our current techniques and ^{135}Ba isobaric interference from the *s*-process component, a higher Cs/Ba phase (^{133}Cs/^{136}Ba > 10), like an evaporate mineral having high Rb/Sr ratio (Zolensky et al. 1999), must be found in primitive solar materials for the detection of ^{135}Ba*.

The ^{87}Rb–^{87}Sr and ^{135}Cs–^{135}Ba decay systems on TL in this study do not provide any chronological information. Is there a possibility that any late events, like an impact metamorphism, disturb the TL chronometers? Considering that the shock stage of TL is typical for carbonaceous chondrite (Brown et al. 2000; Zolensky et al. 2002), it is unlikely that a late impact and the related metamorphism disturbed the TL chronometers. As noted at the end of Section 3.1, the data of Cs/Ba ratios help us to exclude the possibility of terrestrial weathering in our TL sample. A reasonable explanation for the absence of a correlation in the isochron diagrams is a reflection of the fact that Cs and Ba are fractionated via the selective dissolution of Cs from mineral structure due to the relatively higher mobility of Cs compared to Ba during fluid mineral interactions, and that the open system behavior of the ^{135}Cs–^{135}Ba system held in TL during the lifetime of ^{135}Cs. This is supported by the larger variability in the Cs/Ba ratios compared to Rb/Sr ratios shown in Figure 1.

3.4. Isotopic Anomalies of ^{84}Sr, ^{130}Ba, and ^{132}Ba

Variable and detectable isotopic excesses of ^{84}Sr, ^{130}Ba, and ^{132}Ba are observed in L1–3 (see in Tables 2(b) and 3(b)). On the other hand, the L4 fraction shows significant excesses of ^{130}Ba and ^{132}Ba isotopes, but no anomaly of ^{84}Sr.

Yokoyama et al. (2015) found a much wider range of ^{84}Sr isotopic anomalies ($\mu^{84}\mathrm{Sr} = -3427$ to 60) in the TL fractions from their original stepwise-leaching method. In particular, very large ^{84}Sr isotopic deficits were observed in the last leachate ($\mu^{84}\mathrm{Sr} = -3427$). Considering the low Sr elemental abundances (<0.5% of the total Sr content) in the last leachate, the acid-resistant presolar SiC grains might have been enriched by the effective exclusion of the solar Sr component during the leaching processes. On the other hand, the last leachate, L5, in this study still has ~18% of the total Sr content. Comparing the Sr elemental abundance in the last fractions between two

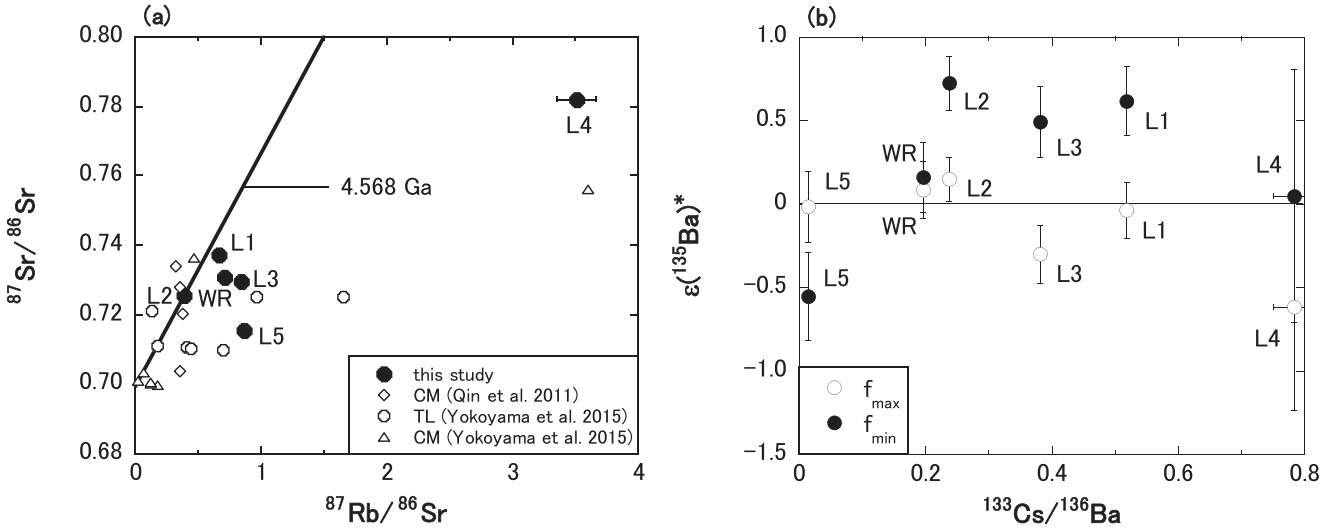

Figure 4. Isochron diagram for (a) ^{87}Rb–^{87}Sr and (b) ^{135}Cs–^{135}Ba, consisting of the L1-5 and WR fractions of the TL meteorite. (a) The line in the figure shows an isochron with an age of 4.568Ga (Bouvier & Wadhwa 2010). For the comparison of other primitive meteorites that experienced aqueous alterations, the data of the leaching fractions of CM and TL are also shown in the figure (CM, Qin et al. 2011; Yokoyama et al. 2015; TL, Yokoyama et al. 2015). (b) The open symbol of $(\varepsilon^{135}Ba)^*$ is the calculated value based on the highest $\varepsilon^{135}Ba/\varepsilon^{137}Ba$ value (f_{max}) in the data of presolar SiC grains (Prombo et al. 1993). The closed symbol is the calculated value based on the lowest $\varepsilon^{135}Ba/\varepsilon^{137}Ba$ value (f_{min}) in the data of the presolar SiC grain (Zinner et al. 1991).

different leaching methods, the small variation of ^{84}Sr of the L5 fraction in this study seems reasonable.

There are three possibilities for the isotopic excess on lighter isotopes of the elements, such as ^{84}Sr, ^{130}Ba, and ^{132}Ba. The first possibility is nucleosynthetic origin for *p*-process isotopes that are produced mainly by type II supernovae (SNe II). Finding anomalies in the pure *p*-process isotope is very rare, although heterogeneous distribution of *p*-process isotopic components in the early solar system has been reported (McCulloch & Wasserburg 1978b; Andreasen & Sharma 2006).

Next, the second possibility is the accumulation of spallogenic nuclides produced by cosmic-ray irradiation. Hidaka & Yoneda (2014) reported systematic *p*-process isotopic excess induced from solar cosmic-ray irradiation, which suggests that this should be discussed further. The Kapoeta meteorite is known as a solar-gas rich meteorite that possibly experienced early irradiation by solar cosmic rays. Systematic isotopic excesses of ^{84}Sr, ^{130}Ba, ^{132}Ba, ^{136}Ce, ^{138}Ce, and ^{144}Sm found in surficial parts of regolith particles of the Kapoeta meteorite suggest the spallogenic nuclides were produced by interaction with a solar cosmic ray from the early Sun. However, considering the cosmic-ray exposure age of TL, the duration of 5.5 Ma (Nakamura et al. 2003) may not be enough to accumulate spallogenic products to be detected by isotopic analysis.

Lastly, the third possibility is apparent anomalies accompanied by enrichment of *s*-process isotopes. Negative or positive anomalies in pairs of ^{130}Ba and ^{132}Ba isotopes are correlated with the excess or deficiency of *s*-process isotopes, which are also found in Ba isotopes of presolar grains and acid-leachates of carbonaceous chondrites (Ott & Begemann 1990; Qin et al. 2011). Figure 5 shows a correlation diagram between $\varepsilon^{130}Ba$ and $\varepsilon^{132}Ba$ to understand the origin of the ^{130}Ba and ^{132}B isotopic excesses found in the TL leachates. The data points of the TL leachates are plotted on the mixing line for solar and presolar components, but off the mixing line for solar and spallogenic components. The results reveal that the isotopic anomalies of ^{130}Ba and ^{132}Ba accompany the *s*-process components. Considering that three of the four Sr isotopes, ^{86}Sr, ^{87}Sr, and ^{88}Sr, are also synthesized by

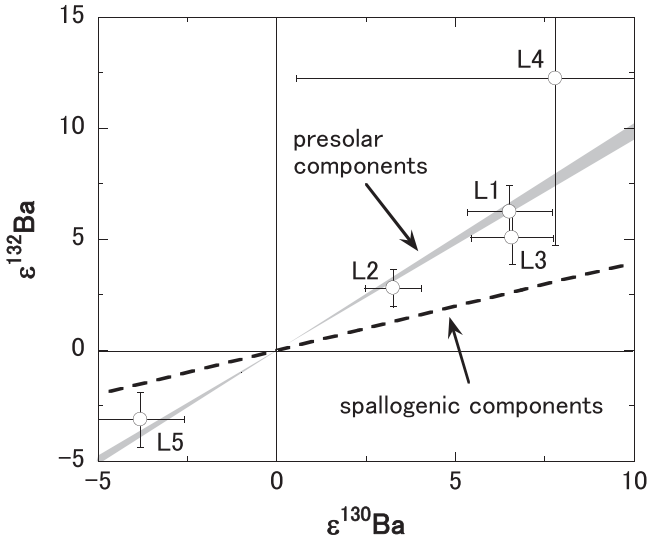

Figure 5. Correlation diagram of $\varepsilon^{130}Ba$ vs. $\varepsilon^{132}Ba$ for isotopic data of this study and the Kapoeta meteorite data. The gray zone shows the mixing zone between the average solar value components and *s*-process components given by presolar SiC grains (Ott & Begemann 1990; Prombo et al. 1993). The dashed line shows spallogenic components given by a previous study (Hidaka & Yoneda 2014).

the *s*-process, the isotopic anomalies of ^{84}Sr found in the L1–3 fractions (see Table 2(b)) are also interpreted as the isotopic shift accompanying the depletion of *s*-process components. It is feasible to consider that the isotopic excesses of ^{84}Sr, ^{130}Ba, and ^{132}Ba in this study are apparent anomalies accompanied by enrichment of *s*-process isotopes, because the normalizing isotopic ratios used in this study, $^{88}Sr/^{86}Sr$ and $^{134}Ba/^{136}Ba$, to make corrections for the instrumental mass fractionation include *s*-process isotopes.

4. Conclusions

The sequential acid-leaching technique was effectively used to separate several fractions in a wide range of Cs/Ba and Rb/Sr elemental ratios and heterogeneous Sr and Ba isotopic

composition from the whole rock of the TL meteorite. The variation of Cs/Ba ratios from the leachates might have been caused by primitive aqueous alteration on the TL parent body, which shows that the Cs/Ba ratio would be a possible indicator to qualify the degree of aqueous alteration. The Ba and Sr isotopic data from the leachates of the TL meteorite indicate the heterogeneous input of additional nucleosynthetic components of s- and *r*-process isotopes into the early solar system. The chronological approaches using ^{87}Rb–^{87}Sr and ^{135}Cs–^{135}Ba decay systems provided unclear results because of the possible redistribution of alkaline elements in association with aqueous alteration. There are at least three potential explanations for the disturbance of the TL chronometers: (1) that the calculations of ^{135}Ba* are not a true reflection of the radiogenic component in the samples; (2) that the successive leaching is more a reflection of selective dissolution of Cs from the mineral structure as compared to Ba, as seen similarly in Rb and Sr; or (3) that the open system behavior of ^{135}Cs–^{135}Ba system held in TL during the lifetime of ^{135}Cs. Finding specific phases with high Cs/Ba elemental ratios in primitive solar materials and the development of higher precision of Ba isotopic analyses than the current technique are required for further discussion about isotopic evidence for ^{135}Cs from Ba isotopic analyses.

Although isotopic anomalies of ^{84}Sr, ^{130}Ba, and ^{132}Ba could be observed in the TL leachates, our systematic isotopic data conclude that their origin is not from the *p*-process isotopic component, but from apparent anomalies accompanying *s*-process isotopic components.

ORCID iDs

Hiroshi Hidaka https://orcid.org/0000-0001-7239-4086

References

A'vila, J. N., Ireland, T. R., Gyngard, F., et al. 2013, GeOCoA, 120, 628
Anders, E., & Grevesse, N. 1989, GeCOA, 53, 197
Andreasen, R., & Sharma, M. 2006, Sci, 314, 806
Andreasen, R., & Sharma, M. 2007, ApJ, 665, 874
Bermingham, K. R., Mezger, K., Desch, S., Scherer, E. E., & Horstmann, M. 2014, GeCOA, 133, 463
Bermingham, K. R., Mezger, K., Scherer, E. E., et al. 2016, GeCOA, 175, 282
Bisterzo, S., Gallino, R., Käppeler, F., et al. 2015, MNRAS, 449, 506
Bouvier, A., & Wadhwa, M. 2010, NatGe, 3, 637
Brandon, A. D., Humayun, M., Puchtel, I. S., & Zolensky, M. E. 2005, GeCOA, 69, 1619
Brennecka, G. A., Borg, L. E., & Wadhwa, W. 2013, PNAS, 110, 17241
Brennecka, G. A., & Kleine, T. 2017, ApJL, 837, L9
Brown, P. G., Hildebrand, A. R., Zolensky, M. E., et al. 2000, Sci, 290, 320
Carlson, R. W., Boyet, M., & Horan, M. 2007, Sci, 316, 1175
Carlson, R. W., Qin, L., & Alexander, C. M. O'D. 2010, LPSC, 41, 2415
Clayton, R. N., & Mayeda, T. K. 2001, LPSC, 32, 1885
Friedrich, J. M., Wang, M., & Lipschutz, M. E. 2002, M&PS, 37, 677
Fujiya, W., Sugiura, N., Hotta, H., Ichimura, K., & Sano, Y. 2012, NatCo, 3, 627
Fujiya, W., Sugiura, N., Sano, Y., & Hiyagon, H. 2013, E&PSL, 362, 130
Hidaka, H., Higuchi, T., & Yoneda, S. 2015, ApJ, 815, 76
Hidaka, H., Ohta, Y., & Yoneda, S. 2003, E&PSL, 214, 455
Hidaka, H., Ohta, Y., Yoneda, S., & DeLaeter, J. R. 2001, E&PSL, 193, 459
Hidaka, H., & Yoneda, S. 2011, GeCOA, 75, 3687
Hidaka, H., & Yoneda, S. 2013, NatSR, 3, 1330
Hidaka, H., & Yoneda, S. 2014, ApJ, 786, 138
Hiroi, T., Zolensky, M. E., & Pieters, C. M. 2001, Sci, 293, 2234
Lodders, K. 2003, ApJ, 591, 1220
MacDougall, J. D., Lugmair, G. W., & Kerridge, J. F. 1984, Natur, 307, 249
McCulloch, M. T., & Wasserburg, G. J. 1978a, ApJ, 220, L15
McCulloch, M. T., & Wasserburg, G. J. 1978b, GeoRL, 5, 599
Nakamura, T., Noguchi, T., Zolensky, M. E., & Tanaka, M. 2003, E&PSL, 207, 83
Nier, A. O. 1938, PhRv, 54, 275
Ott, U., & Begemann, F. 1990, ApJ, 353, L57
Prombo, C. A., Podosek, F. A., Amari, S., & Lewis, R. S. 1993, ApJ, 410, 393
Qin, L., Carlson, R. W., & Alexander, C. M. O'D. 2011, GeCOA, 75, 7806
Sanchez, A. L., Smolders, K., Van den Brande, K., et al. 2002, J Environ Radioactiv, 63, 35
Savina, M. R., Davis, A. M., Tripa, C. E., et al. 2003, GeCOA, 67, 3201
Sheppard, S., Long, J., Sanipelli, B., & Sohlenius, G. 2009, Solid/liquid partition coefficients (Kd) for selected soils and sediments at Forsmark and Laxemar–Simpevarp SKB Report R-09-27
Shima, M., & Honda, M. 1967, E&PSL, 2, 337
Tomeoka, K., & Buseck, P. R. 1985, GeCOA, 49, 2149
Vernazza, P., Fulvio, D., Brunetto, R., et al. 2013, Icar, 225, 517
Yokoyama, T., Fukami, Y., Okui, W., Ito, N., & Yamazali, H. 2015, E&PSL, 416, 46
Yoneda, S., Ebihara, M., Oura, Y., et al. 2001, LPSC, 32, 2034
Zinner, E., Amari, S., & Lewis, R. S. 1991, ApJ, 382, L47
Zolensky, M. E., Bodnar, R. J., Gibson, E. K., et al. 1999, Sci, 285, 1377
Zolensky, M. E., Boucier, W. L., & Gooding, J. L. 1989, Icar, 78, 411
Zolensky, M. E., Nakamura, K., Gounelle, M., et al. 2002, M&PS, 37, 737